CO9-1   Solid phase transformation of tetravalent metal hydroxide at elevated temperatures

T. Kobayashi, Y. Sato, T. Suzuki, T. Sasaki, K. Mori[1], K. Takamiya[1]

Graduate School of Engineering, Kyoto University
[1] Institute for Integrated Radiation and Nuclear Science, Kyoto University

INTRODUCTION: For the reliable prediction of radionuclide migration behavior under relevant radioactive waste disposal conditions, it is necessary to establish a thermodynamic model on the solubility limits of radionuclides in groundwater. Several actinides and long half-life fission products such as ^{93}Zr are known to exhibit a tetravalent oxidation state in repository systems and easily precipitate as an amorphous hydroxide ($M(OH)_4(am)$) due to strong hydrolysis reactions. Although the solubility is primarily controlled by the amorphous hydroxide, $M(OH)_4(am)$ is thermodynamically meta-stable, and can be converted to stable crystalline oxide of $MO_2(cr)$ by heating or calcinations [1]. Since the decay heat emissions are transferred to the groundwater surrounding the waste packages, the repository systems are expected to be under elevated temperature conditions [2]. Therefore, it is important to reveal an impact of elevated temperature on the solid phase transformation of $M(OH)_4(am)$ for the prediction of the solubility limits of radionuclides in tetravalent oxidation state. On the other hand, a number of literatures have investigated the solubility of $MO_2(cr)$ and several studies suggested that the surface of $MO_2(cr)$ are possibly hydrolyzed to form hydroxide layer, which is controlling the apparent solubility [3]. Since the solubility product (K_s) of $MO_2(cr)$ and $M(OH)_4(am)$ differs more than several orders of magnitude, it is of importance to clarify the solid phase transformation between $MO_2(cr)$ and $M(OH)_4(am)$ for establishing the robust thermodynamic model on the solubility of radionuclides in tetravalent oxidation state.

In the present study, we focused Zr as one of the fission products in tetravalent oxidation state under the repository conditions. $ZrO_2(cr)$ powder were first measured by a versatile compact neutron diffractometer (VCND) at the B-3 beam port of KUR as references. Then the neutron diffraction patterns of amorphous zirconium deuterium hydroxide ($Zr(OD)_4(am)$) aged at 25 to 90 ºC were collected to investigate a temperature effect on the transformation of $ZrO_2(cr)$ and $Zr(OD)_4(am)$.

EXPERIMENTS: The powder samples of $ZrO_2(cr)$ was purchased from WAKO Pure Chem. and put in sample holders without further treatment. The samples of $Zr(OD)_4(am)$ was prepared by an oversaturation method. A few grams of $ZrCl_4$ (WAKO Pure Chem.) was dissolved in D_2O to prepare the Zr stock solution ($[Zr]$ = 0.2 M). Portions of deuterium hydroxide (NaOD) were then added in the stock solution to adjust the pHc at pHc = 2.7. The sample suspensions were placed in ovens kept at 25, 40, 60, and 90 ºC for 3 weeks. After the aging periods at each temperature, the pHc of the sample solutions was measured. The solid phases were separated by centrifugation and dried in vacuum desiccator. After the dryness, the powder samples were put in sample holders and measured by a VCND installed at the B-3 beam port of KUR. A Cu monochromator with 40 mm diameter was used to monochromatize the neutron wavelength of 1.0Å. The beam size was approximately 10 mm in width and 30 mm in height. The beam flux was 1.3×10^5 n/s·cm^2 during the operation at the power of 5 MW on KUR.

RESULTS: Figure 1 shows the neutron diffraction (ND) pattern of $ZrO_2(cr)$ in comparison with the X-ray diffraction (XRD) patterns [1]. The ND patterns exhibited intense peaks at low d ($d = \lambda/2 \sin \theta$), while the peaks in the XRD patterns showed less intensities. The peak positions of both methods agreed and indicated the monoclinic structure of $ZrO_2(cr)$.
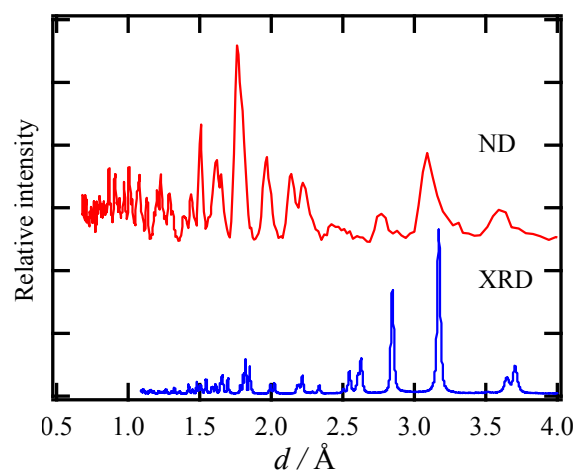

Fig. 1 Neutron diffraction (ND) and X-ray diffraction (XRD) patterns of $ZrO_2(cr)$.

The neutron diffraction pattern of $Zr(OD)_4(am)$ after aging at 25 ºC showed a halo pattern typical for amorphous phase. With increasing the aging temperatures, the peaks corresponding to $ZrO_2(cr)$ appeared and those after aging at 90 ºC became clear with large intensities, indicating the progress of crystallization by heating. Further investigation is planned by an undersaturation approach from $ZrO_2(cr)$, and also for other elements in tetravalent oxidation state.

REFERENCES:
[1] T. Kobayashi *et al.* Langmuir **35**, (2019) 7995.
[2] JNC Report TN1410 2000-001; JNC: Tokai, Japan, (2000).
[3] D. Rai *et al.*, Radiochim. Acta **79**, (1997) 239.

R2018

CO9-2　　　　Deterioration of simulated fuel debris in aqueous environment

T. Sasaki, R. Tonna, N. Sato[1], A. Kirishima[1], D. Aki-yama[1], T. Kobayashi, K. Takamiya[2], S. Sekimoto[2]

Graduate School of Engineering, Kyoto University
[1] *Institute of Multidisciplinary Research for Advanced Materials, Tohoku University*
[2] *Institute for Integrated Radiation and Nuclear Science, Kyoto University*

INTRODUCTION:
The fuel debris generated by the accident at the Tokyo Electric Power Company (TEPCO) Fukushima Daiichi Nuclear Power Station (FDNPS) is still in contact with water, and it deteriorates over time with the dissolution of nuclides due to a solid-liquid reaction on the debris surface. Since it takes a long time to plan an extraction method of the debris from the plant, it is essential to accumulate basic knowledge for predicting changes of the chemical property of debris, but there are few knowledges about debris containing UO_2, zircaloy, and structural materials such as SUS304 stainless steel (SUS).

In order to simulate the dissolution behavior of nuclides from 1F debris, we have some prepared alloy-based debris samples and focused the elution behavior of uranium and fission products (FPs). Two evaluation methods are adopted in this study. One is an addition method in which non-radioactive elements (as cold FPs) were added to a sample in advance. The other is an irradiation method. The debris sample was irradiated with short-time thermal neutrons to produce FPs.
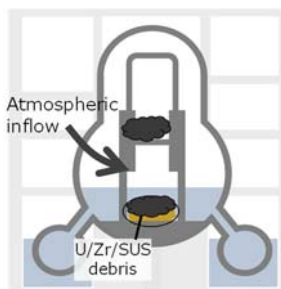

Fig.1 Schematic overview of 1F core melting

EXPERIMENTS:
A powder mixture of UO_2 obtained by hydrogen reduction of U_3O_8 and SUS was heated in an oxidizing atmosphere (2% O_2 + 98% Ar, 1200 °C) to prepare simulated debris, and a powder XRD was adopted. The representative solid phases are follows; #XO (U_3O_8 (A)), #ZO ($A+U_{1-y}Zr_yO_{2+x}$), #SO ($A+U(Fe)CrO_4$), #FO (A), #CO ($A+UCrO_4$), which were prepared from UO_2 (B), B+ZrO_2, B+SUS, B+Fe, B+Cr, respectively.

The solid-phase sample sealed in a quartz ampoule was inserted into a polyethylene capsule and irradiated using Pn-2 of Kyoto University Reactor. FPs are ^{137}Cs, ^{131}I, ^{140}Ba, ^{103}Ru, ^{95}Zr (irradiation method), Cs, Sr, Eu (addition method). After contacting the sample with 0.1 M $NaClO_4$, pure water, and artificial seawater at 25 °C, the nuclide concentration before and after the immersion was determined by γ-ray spectroscopy and ICP-MS for in the irradiation method and the addition method, respectively. The cumulative γ radioactivity of nuclide M dissolved during a given period was determined by considering a decay correction, in accordance with the method used. The leaching ratio (r_M) is defined as

$$r_M = A_{f,M} \exp\left(\frac{t\ln2}{t_{1/2}}\right)/A_{i,M} \qquad (1)$$

where $A_{i,M}$ expresses the initial inventory (Bq) of M initially present in the solid solution sample, $A_{f,M}$ expresses the radioactivity (Bq) in the filtrate measured after the leaching period (t), and $t_{1/2}$ expresses the half-life of the nuclide. In the addition method, since a cold FP partly volatilized during heat treatment, the sample was dissolved by acid to correct the inventory. For uranium and cold-FPs, the unit of Bq is replaced by mole. R_M corresponds to r_M/r_U and is the dissolution ratio of M normalized by that of uranium.

RESULTS:
In the samples #XO, #ZO and #SO, Cs was preferentially leached over U, immediately after immersion in both the irradiation method and the addition method ($R_{Cs}\approx10^3$), and then the R_{Cs} value decreased with time. It was suggested that easily soluble nuclides on the surface of the solid phase could leach immediately just after immersion of sample, but after that, matrix uranium dissolution might become a rate-determining reaction. It was found that divalent Ba (irradiation method) and Sr (addition method) same as in Cs leached preferentially over U, while a trivalent Eu showed a strong tendency for a harmonized dissolution with U. Thus, the addition method could provide the knowledge of trivalent ions. The r_U was in the order of pure water << Na perchlorate solution < seawater, and the influence of anion-U complex formation contained in the liquid phase was observed. At this time, R_{Cs} and R_{Sr} tended to be pure water >> Na perchlorate solution > seawater, while R_{Eu} was in the order of pure water < Na perchlorate, seawater, depending on the valence of the ions.

REFERENCES:
[1] V. Almjashev et al., Radiochem. **53** (2011) 13.
[2] X. Guo et al., Dalton Transactions **45** (2016) 4622.
[3] H. Ikeuchi et al., J. Nucl. Sci. Technol. **51** (2014) 996.
[4] B. Sailaja et al., Physical Sciences **74** (2004) 399.

R2019

CO9-3   The solvent extraction behavior of Antimony in nitric acid solution using TDdDGA

Y. Nakamura[1], S. Ogawa, S. Takahashi, C. Kato, S. Fukutani[1], T. Matsumura[2], H. Suzuki[2], and T. Fujii

Graduate School of Engineering, Osaka University
[1]Institute for Integrated Radiation and Nuclear Science, Kyoto University
[2]Nuclear Science and Engineering Center, Japan Atomic Energy Agency

INTRODUCTION: ^{125}Sb, an isotope of antimony (Sb), is a fission product (FP) nuclide in the high-level liquid waste and understanding its extraction behavior is crucial for the reprocessing be highly active liquid waste. Although the amount contained in the nuclear waste is relatively small compared to other elements (0.026 mM for a synthetic solution [1]), its short half-life of 2.76 years [2] is problematic and therefore the influence of Sb should be considered. *N,N,N',N'*-tetradodecyldiglycolamide (TDdDGA) is an extractant synthesized at Japan Atomic Energy Agency (JAEA) for the recovery of minor actinides (MA) and rare earth elements (REE) from the high-level liquid waste, but the extraction behavior of Sb has not been studied using this extractant. In this study, the solvent extraction behavior of Sb by TDdDGA and its dependency on nitric acid solution and also the separation factor from neodymium (Nd), a REE, were studied and determined.

EXPERIMENTS: For the HNO_3 concentration dependency, TDdDGA was used as the extractant and a mixed solution of n-dodecane and 1-octanol was used as solvents to adjust the TDdDGA concentration to 0.1 M. A Sb shot was placed in 7 M HNO_3 for 18 hours at room temperature to dissolve and then diluted to form the HNO_3 concentration of 0.1, 0.2, 0.5, 1, 1.5, 2, 3, 4, 5 M. Both phases were stirred for 30 mins to reach equilibrium. The solution was separated by centrifugation and the aqueous phase was exchanged with a 0.1 M HNO_3 and back extraction was performed. For the Nd separation experiment, the concentration of Nd and Sb were adjusted to be the same in a 1 M and 3 M HNO_3 solution for the aqueous phase. The organic phase was 0.1 M TDdDGA diluted by n-dodecane and 1-octanol. All experiments were carried out at room temperature. The Sb and Nd concentration of the aqueous phase before and after both extractions were measured by Inductively Coupled Plasma-Atomic Emission Spectrometry (ICP-AES) and Inductively Coupled Plasma-Mass Spectrometry (ICP-MS) at the Institute for Integrated Radiation and Nuclear Science, Kyoto University, and the distribution ratios and separation factors were determined.

RESULTS AND DISCUSSIONS: The results for the HNO_3 dependency are shown in Fig. 1. For the concentrations above 0.5 M HNO_3, from slope analysis, there is a slope 1 positive correlation between the distribution ratio and HNO_3 concentration. On the other hand, below 0.5 M HNO_3, there was no correlation. This suggests that
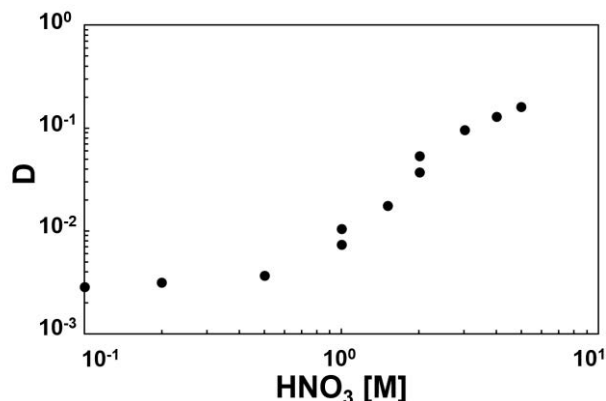

Fig. 1.   Dependence of D on nitric acid concentration for Sb.

1) Sb and TDdDGA form a compound in a 1:1 ratio from HNO3 concentrations greater than 0.5 M and 2) the oxidation state of Sb changes around 0.5 M, due to the HNO_3 concentration. The possible ligands that can form at the HNO_3 concentrations used in this study is SbO_2^+, SbO^+, $HSbO_2$ and $Sb(OH)_6$- [3] which are either Sb(III) or Sb(V). This supports the observation of the correlation change at 0.5 M HNO_3.

The separation factor for Sb/Nd was 6.8×10^3 and 9.1×10^3 for 1M and 3M HNO_3 respectively. Furthermore, the distribution ratios of Sb (1M: 0.0054, 3M: 0.086) of and Nd (1M: 36.7, 3M: 786) show that the Sb and Nd can be clearly separated into different phases. Compared with TODGA [4], separation of Sb from a trivalent lanthanide or actinide element is efficient using TDdDGA.

CONCLUSIONS: The extraction behavior of Sb in varying nitric acid concentrations using TDdDGA was studied by using the solvent extraction method. The separation factor of Sb and Nd was also determined. Sb and TDdDGA had a 1:1 bond for HNO_3 concentrations of 0.5 M and above. TDdDGA is an efficient extractant to separate Sb from trivalent F block elements.

REFERENCES:
[1] Savantesson I. *et al.*, J. Inorg. Nucl. Chem., **41** 383-389 (1979).
[2] Meija J. *et al.*, Pure Appl. Chem., **88** 3 293-306 (2016).
[3] Pitman A. L. *et al.*, J. Electrochem. Soc., **104** 10 594-600 (1957).
[4] Zhu Z.-X *et al.*, Anal. Chim. Acta., **527** 2 163-168 (2004).

R2063

CO9-4   Electrochemical behavior of U^{3+} on Ru electrode in LiCl-KCl melts

T. Murakami[1], Y. Sakamura[1], K. Uozumi[1], M. Iizuka[1], and K. Takamiya[2]

[1]Central Research Institute of Electric Power Industry
[2]Institute for Integrated Radiation and Nuclear Science, Kyoto University

INTRODUCTION: Actinides form alloys with noble metal fission products during the irradiation of metallic fuel [1]. To understand the detailed behavior of actinides during electrorefining process of the irradiated metallic fuel, it is necessary to accumulate the basic knowledge on the electrochemical properties of the actinides-noble metal alloys. This study focused on U-Ru alloy and investigated the electrochemical behavior of U-Ru alloy in LiCl-KCl-UCl_3 melts at 773 K.

EXPERIMENTS: Electrochemical measurements were performed in an Ar atmosphere glove box. LiCl-KCl eutectic salt containing 0.16 mol% UCl_3 was melted at 773 K and used as the electrolyte. The working electrode was a Ru metal plate electrode (1mm×2mm×7mm (immersion depth into the melt), 99.5 % purity, Nilaco) or a W wire electrode (1 mmφ, 3 mm immersion depth into the melt). The counter electrode was a glassy carbon rod. Another W wire was used as the quasi reference electrode, of which potential was calibrated to Ag/AgCl reference electrode potential periodically.

RESULTS: Cyclic voltammogram of the W electrode in the LiCl-KCl-UCl_3 melts showed a cathodic (c1) and anodic (a1) current couple ascribing to U metal deposition and dissolution, respectively, at around -1.4 V (vs. Ag/AgCl) as seen in Fig. 1(a),

$$U^{3+} + 3e^- \rightleftarrows U \qquad (1)$$

In the cyclic voltammogram of the Ru electrode (Fig. 1(b)), cathodic current peaks (c2 and c3) were observed at more positive potential than that of U metal deposition (c1). Taking into account that five alloy phases, U_2Ru, URu, U_3Ru_4, U_3Ru_5 and URu_3, exist in U-Ru binary system [2], the cathodic current peaks, c2 and c3, were considered to be due to U-Ru alloy formation,

$$U^{3+} + xRu + 3e^- \rightarrow URu_x \qquad (2)$$
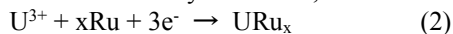
During the anodic scan in Fig. 1(b), an anodic current peak a4, a broad anodic current peak a3 and an anodic current peak with a shoulder a2 were found, which might have corresponded to U dissolution from the U-Ru alloy. For the purpose of determining the U-Ru alloy formation and deformation potentials in detail, a galvanostatic electrolysis at 0.1 mA was conducted using the Ru electrode on which U metal had been deposited by a potentiostatic electrolysis at -1.44 V for 10 s. As seen in Fig. 2, the potential of the Ru electrode was initially that of the deposited U metal. Then, the potential shifted to a positive direction along with time, showing several potential plateaus. A different pair of two U-Ru alloy phases should exist on the surface of the electrode at each potential plateau. Similar electrochemical measurements will be

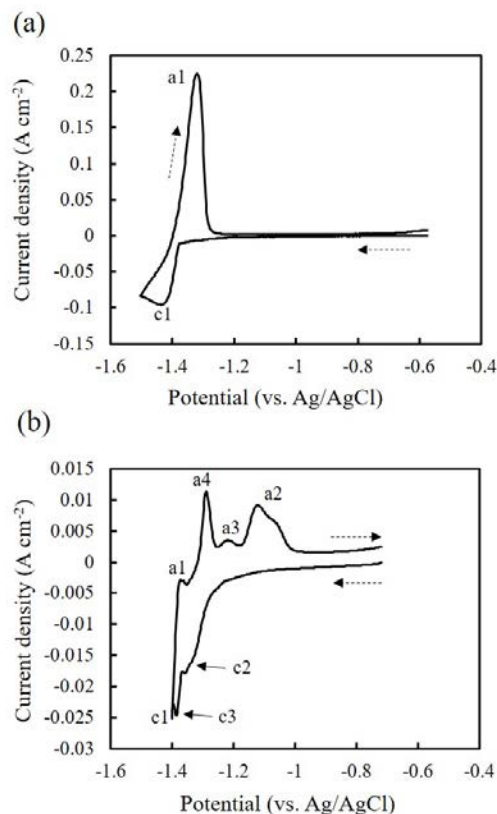carried out at different temperature to obtain thermodynamic properties of U-Ru system.

Fig. 1 Cyclic voltammograms of (a) W and (b) Ru electrodes in LiCl-KCl-0.16mol%UCl_3 melts at 773 K. Scan rate was 50 mVs^{-1}.
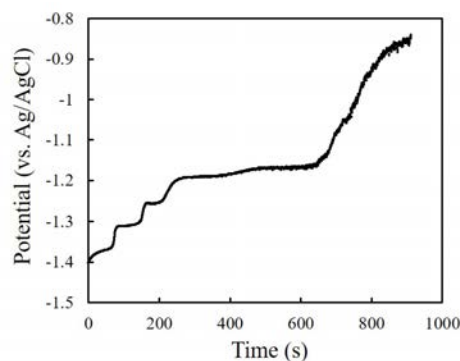

Fig. 2 Potential change of Ru electrode during galvanostatic electrolysis at 0.1 mA after U had been deposited on the Ru electrode by a potentiostatic electrolysis at -1.44 V for 10 s at 773 K.

REFERENCES:
[1] K. Inagaki *et al.*, Trans. Am. Nucl. Soc., **110** (2014) 786-787.
[2] T. B. Massalski ed., BINARY ALLOY PHASE DIAGRAMS SECOND EDITION, ASM International (1990).

R2091

CO9-5   Coprecipitation of Ca, Sr, Ba, and Ra with barium sulfate toward the chemical study of Nobelium

S. Hayami, Y. Kasamatsu, E. Watanabe, R. Nakanishi, K. Sawamura, K. Takamiya[1], and A. Shinohara

Graduate School of Science, Osaka University
[1]Institute for Integrated Radiation and Nuclear Science, Kyoto University

INTRODUCTION: Nobelium (No) with atomic number 102 is one of actinide elements. It is reported that stable oxidation state of No is +2 although those of the other heavy actinide elements are all +3. The chemical behavior of No is reported to be similar to that of group 2 elements in HCl [1]. However, it is difficult to investigate the chemical properties of No because of low production rates and short half-lives of the No nuclides. Fundamental experiments of group 2 elements for various chemical reactions are needed to establish new chemical experiments for No.

Previously, we reported new experimental method in which the hydroxide complexation of the target elements can be studied from the coprecipitation behavior with samarium hydroxide [2]. So far, we have qualitatively investigated the coprecipitation behaviors of various elements, and we successfully applied the method to element 104, rutherfordium (Rf) [3]. In this study, in order to elucidate the new chemical properties of No, we focused on the reaction with sulfate ions, and experimentally investigated the coprecipitation behavior of group 2 elements: Ca, Sr, Ba, and Ra, with $BaSO_4$ using ammonium sulfate in addition to sulfate precipitation behavior. Suitable experimental conditions for coprecipitation experiment of No were determined.

EXPERIMENTS: ^{85}Sr and ^{133}Ba samples were prepared by irradiating protons on pellet samples of RbCl for 1 h and of CsCl for 10 h using the AVF cyclotron at RCNP. ^{47}Ca sample was prepared by irradiating thermal neutrons (3×10^{13} cm^{-2} s^{-1}) on a powder sample of CaO for 1 h using the reactor at KURNS. They were separated from other majority of radioisotopes by cation-exchange and anion-exchange methods. ^{226}Ra tracer was used to investigate the behavior of Ra.

In the coprecipitation experiment, 20 μL (20 μg) of $BaCl_2$ solution was added into the RI tracer solution. In case of the precipitation experiment, 20-1000 μg of Sr or Ba chloride or ~10 mg of ^{47}CaO in aqueous solution was added. After mixing it, 2 mL of ammonium sulfate solution was added to generate sulfate precipitate. Then, these solutions (0.0010–2.0 M) were stirred for 5 min at room temperature. The precipitate was collected on a membrane filter by suction filtration. The precipitate and filtrate samples were subsequently dried on heater at 100 degree C, and were assayed by γ-ray measurements. The (co)precipitation yields were determined from the radioactivities of the γ rays counted.

RESULTS: The precipitation and coprecipitation yields were determined from the equation: A_{ppt} / (A_{ppt} + A_{fil}), where A represents the radioactivity, and ppt and fil indicate the precipitate and filtrate, respectively.

The coprecipitation behavior of Sr and Ba was basically consistent with that in precipitation, suggesting that sulfate precipitation (complexation) properties of the group 2 elements can be investigated based on their sulfate coprecipitation behavior. The coprecipitation yields of Ca, Sr, Ba, and Ra are shown in Fig.1. The yield increases with an increase of the atomic number; namely, ionic radius, and this trend is qualitatively consistent with that in their solubility products. The ionic radius of No is between Ca and Sr and thus, the yields of No might be between those of Ca and Sr. Maybe, due to the influence of strong relativistic effects on the orbital electrons in No, No will show different behavior from a simple prediction based on the tendency among group 2 elements. It is very intriguing to experimentally investigate the sulfate coprecipitation behavior of No with barium sulfate.
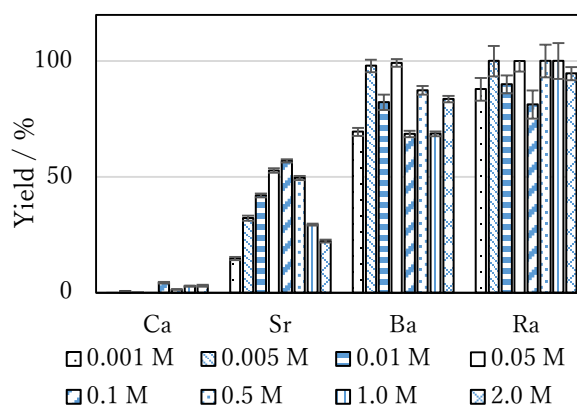

Fig. 1. The yields in sulfate coprecipitation experiment.

REFERENCES:
[1] R. J. Silva *et al*., J. Inorg. Chem., **13**, 9, 2233-2237 (1974).
[2] Y. Kasamatsu, *et al*., Appl. Radiat. Isot. **118**, 105-116 (2016).
[3] Y. Kasamatsu, *et al*., Nature Chem. **13**, 226–230, (2021).

R2129

CO9-6
Electrostatic Interaction between Fission Products and Solution Aerosol Particles in Radioaerosol Generation Process

K. Takamiya, T. Takeuchi, M. Inagaki, S. Sekimoto, Y. Oki and T. Ohtsuki

Institute for Integrated Radiation and Nuclear Science, Kyoto University

INTRODUCTION: One of the major forms which had spread radioactive materials in the environment at the severe accident of Fukushima Daiichi Nuclear Power Plant (FDNPP) is radioactive aerosol. Radioactive cesium and other radio isotopes released from the plant were transported by aerosol particles [1]. Part of the radioaerosol particles containing fission products were generated in the reactor building. Fission products released from nuclear fuels by high temperature might attach to surface of aerosol particles to generate radioaerosol particles. The generation processes of the radioaerosol particles are important to understand surrounding condition of nuclear fuels. Experimental approach to elucidate the generation process of the radioactive aerosols has been performed in our previous work [2-5]. In the present work, the attachment behavior of fission products to solution aerosol particles has been observed using neutron irradiated UO_2 powder as a source of fission products. Fission products released from the irradiated UO_2 by heating move with thermal velocity and might attach to surface of aerosol particle by electrostatic interaction.

EXPERIMENTS: The experimental method to generate and collect radioactive aerosol particles containing fission products is shown in the previous report [5]. Powder of UO_2 was encapsulated in a quartz tube under reduced pressure, and the quartz tube covered by a polyethylene tube was inserted into polyethylene capsule to irradiate neutrons using pneumatic transport system, Pn-2, at the power of 1MW on KUR. The amount of UO_2 was 10 mg, and the neutron irradiation time was 5 min. A few mg of irradiated UO_2 powder was extracted to another quartz tube placed in an electric furnace within 60 min after the irradiation. Fission products produced in the irradiated UO_2 powder was released by heating the furnace up to 1000°C. On the other hand, atomizer filled with 0.01 M solution generate solution aerosol particles. Four kinds of solution; sodium chloride, sodium bromide, sodium iodide and ammonium sulfate, were used in the present work. Both released fission products and solution aerosol particles were aspirated by a suction pomp to inject into a cylindrical chamber. Radioactive aerosol particles were generated by attaching fission products to aerosol particles in the chamber, and the difference of interaction time causes the difference of effective surface area of aerosol particles to attach fission products. The produced radioactive aerosol particles were collected on a polycarbonate filter at downstream of the chamber. The amount of fission products which was attached to aerosol particles were estimated by gamma-ray spectrometry for the filter using a Ge-detector (Canberra, GC2020). On the other hand, the total amount of fission products released from the irradiated UO_2 powder by heating was estimated by subtraction of gamma-ray spectra measured before and after release of fission products by heating.

RESULTS: The attachment ratio of short half-lived fission products; $^{91,92}Sr$, ^{138}Cs, $^{134,135}I$, ^{134}Te and ^{128}Sn, to NaCl, NaBr, NaI and $(NH_4)_2SO_4$ solution aerosol particles is estimated in the present work and shown in Figure 1. The attachment ratio of Sr isotopes is not shown in the figure because the ratio was below the detection limit. The varieties of attachment ratio of each nuclide to different solution aerosol are around one order. On the other hand, the differences of the ratio among nuclides to the same solution aerosol is up to three order. The result indicates that the attachment ratio depends on the chemical properties of fission products released from UO_2 more than those of solution aerosol particles. The fission products of $^{91,92}Sr$, ^{138}Cs and $^{134,135}I$ are isotopes of important radionuclides; ^{90}Sr, $^{134,137}Cs$ and $^{131,133}I$, which had been released from FDNPP and affected high dose rate in the environment. The result will contribute to the severe accident simulation in the aspect of estimating the radioactivity released from the power plant.
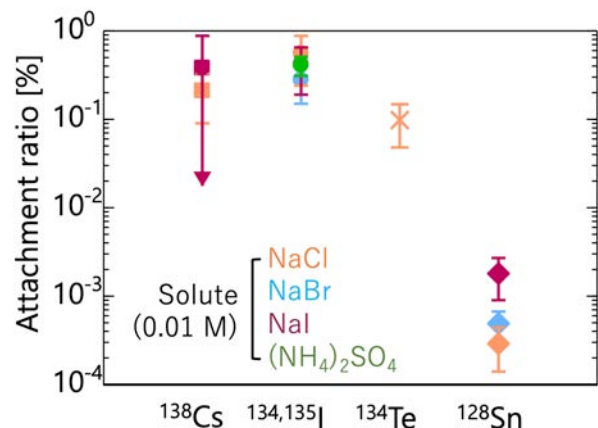

Fig. 1 Attachment ratio of five fission products to four different solution aerosol particles.

REFERENCES:
[1] N. Kaneyasu et al. Env. Sci. Technol. **46**(11), 5720–5726 (2012).
[2] K. Takamiya et al., J. Radioanal. Nucl. Chem. **307** (2016) 2227-2230.
[3] K. Takamiya et al., J Radiat. Prot. Res. **41** (2016) 350–353.
[4] K. Takamiya et al., KURRI Progress Report 2017 (2018) 13-13.
[5] K. Takamiya et al., KURNS Progress Report 2018 (2019) 95-95.

R2141